FERMILAB-CONF-05-581-E

Recent results from the Tevatron

C. Royon

DAPNIA/Service de physique des particules, CEA/Saclay, 91191 Gif-sur-Yvette cedex, France
and Fermi National Accelerator Laboratory, Batavia, Illinois 60510, USA

In these lectures, we describe some recent results from the DØ and CDF experiments at the Tevatron.

1. Introduction and description of DØ and CDF experiments

In this article, we will describe some of the newest results obtained by the DØ and CDF experiments at the Tevatron in 2005. We will give in turn some results about QCD, top, b physics, new phenomena and prospects for Higgs boson searches.

The Tevatron is a $p\bar{p}$ collider located near Chicago with a center-of-mass energy of 1.96 TeV, which is the highest energetic machine before the start of the LHC. The expected sensitivity to physics beyond the standard model is thus high. The two main experiments (DØ and CDF) are installed along the ring and provide independent physics analyses to allow cross checks between the results.

The accumulated luminosity [1] by the DØ experiment is given in Fig. 1 until the time of the Summer school. The expected luminosity before 2009 when the Tevatron will probably be turned off is expected to be between 4 and 8 fb^{-1}. The luminosity accumulated by the CDF experiment is found to be similar and slightly higher. The data taking efficiency, which gives the percentage of time when DØ is able to take data, is noticeably well above 90%.

A scheme of the DØ detector is given in Fig. 2. We will give the description of the DØ detector starting from the center to the outside [1]. The most central part comprises a (forward and central) silicon and a fiber tracking detector, which allows to measure precisely the location and momentum of

[1] The luminosity is directly related to the number of events which have been taken by the experiment, since $N = \sigma \times \mathcal{L}$ where N, σ, and $\mathcal{L}$ are respectively the number of events for a given process, the cross section for that process and the luminosity.

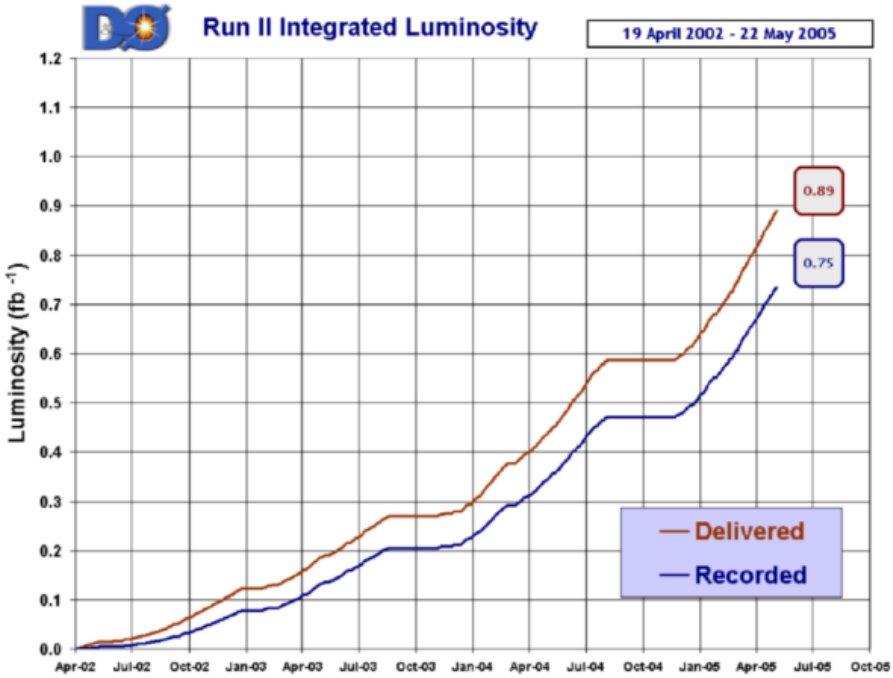

Fig. 1. Integrated luminosity accumulated by the DØ experiment.

charged particles. The tracking detector is surrounded by a solenoid which delivers a magnetic field of 2 T. The compensating, finely segmented, liquid argon and uranium calorimeter provides nearly a full solid angle coverage up to a rapidity larger than 4. The muon detector is composed of the central muon proportional drift tubes, scintillating detectors used in the trigger, and mini-drift tubes in the forward region, allowing a muon detection up to a rapidity of 2. A toroid magnet allows to reconstruct the muon momentum using the muon system only, and a better resolution is obtained by combining this information with the ones from the tracking detectors. The CDF detector has similar performances and is composed of a central tracking and silicon detector, a calorimeter made of lead sheets sandwiched with scintillator for the electromagnetic part, and of iron plates and scintillator for the hadronic part, and a muon detector. The leveir arm for the tracking detector is larger than for DØ because of the space availability (we recall that DØ did not have any central magnet in Run I).

We will now describe the different physics results in turn.

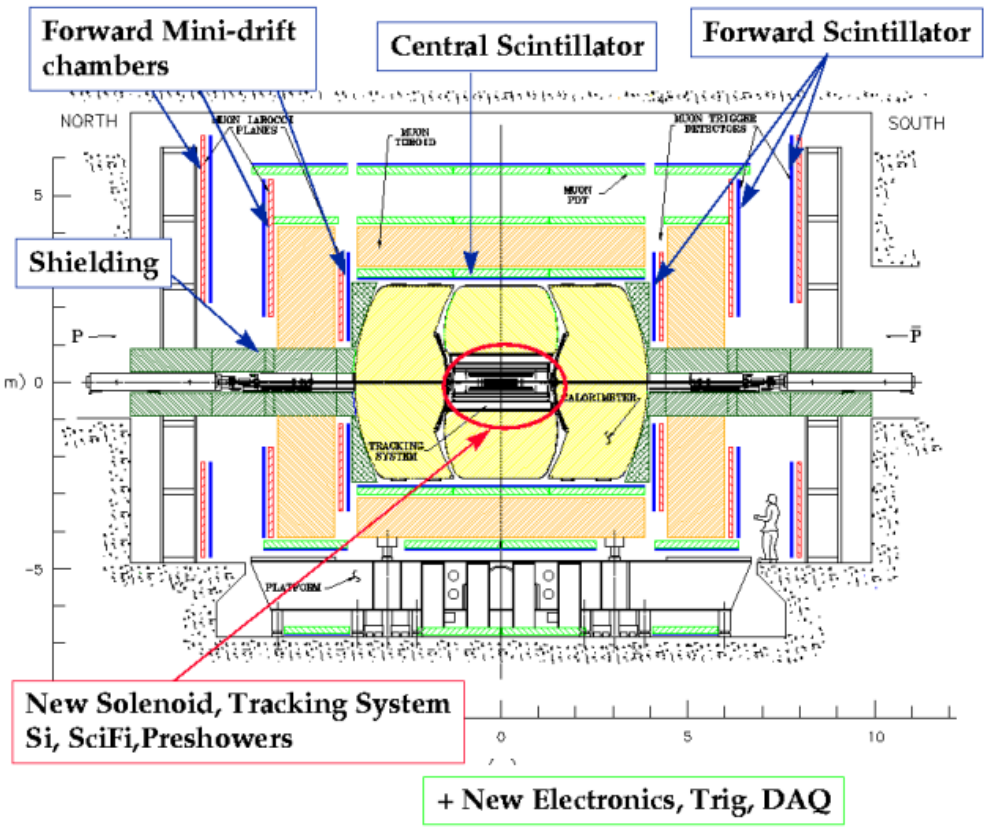

Fig. 2. Scheme of the DØ detector.

2. Results on QCD

2.1. Why measuring the QCD cross sections at the Tevatron?

In this paragraph, we will discuss the CDF and DØ results on QCD. First, it is useful to notice that these experiments lead to results quite complementary to the ones from HERA, and the previous fixed target experiments. As shown in Fig. 3, the kinematical plane in (x, Q^2) (x is the proton momentum fraction carried by the interacting quark, and Q^2 is the squared energy transferred at the lepton vertex) reached at HERA extends noticeably the reach of the previous fixed target experiment. The Tevatron experiments are also sensitive to higher Q^2 and higher x value. The con-

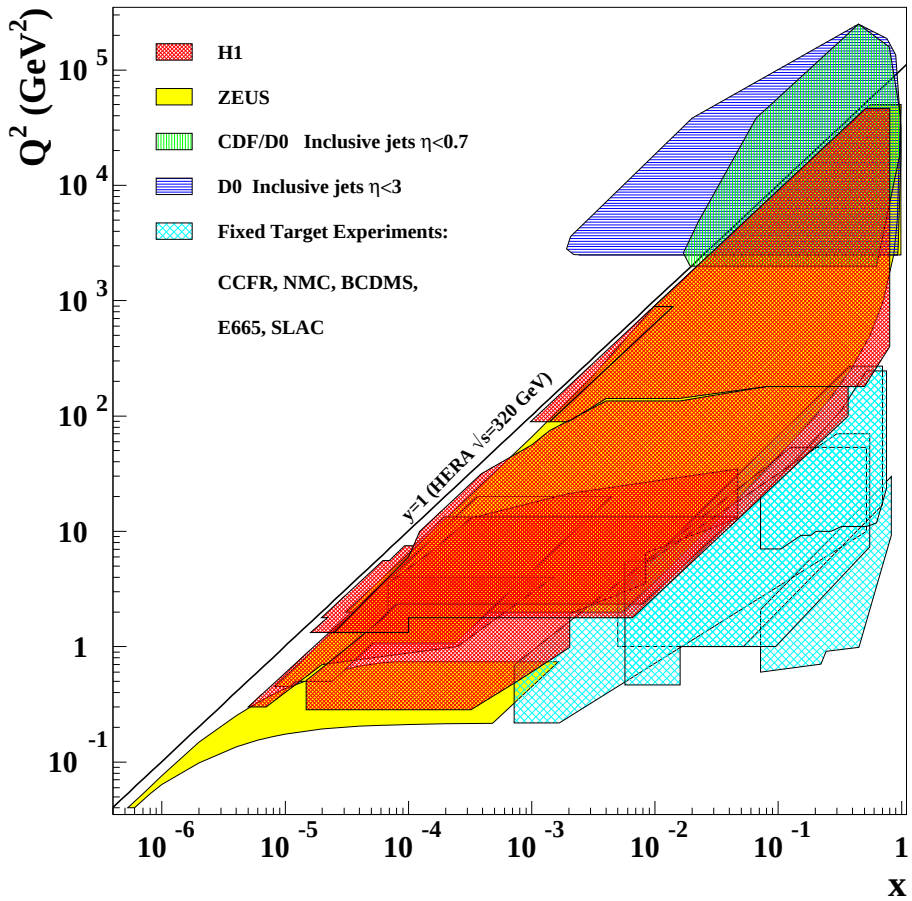

Fig. 3. Kinematic plane in (x, Q^2) reached by Tevatron, HERA and the fixed target experiments.

straint on the gluon density at high x in particular is coming mainly from the Tevatron and fixed targets experiments. In that sense, the data taken at HERA and Tevatron are complementary to obtain precisely the quark and gluon densities from Dokshitzer Gribov Lipatov Altarelli Parisi (DGLAP) QCD fits [2]. The F_2 structure function measurements as well as the QCD fits are given in Ref. [3]. The uncertainty on the gluon distribution at high x is large and reaches more than 50% for x larger than 0.5.

2.2. QCD inclusive jet cross section measurements

The CDF and DØ experiments performed a preliminary measurement of the inclusive jet cross sections as a function of their transverse momentum to probe the high-x gluon density. The preliminary measurement performed by the DØ collaboration with a luminosity of about 378 pb^{-1} and two bins in rapidity is given in Fig. 4. The measurement in the lowest bin in rapidity ($|y| < 0.4$) has been multiplied by 10 to be able to distinguish between both measurements. The data are compared with NLO calculations using the CTEQ6.1M parametrisation [5] and the NLOJET++ program [6]. There is a good agreement between the measurement and the QCD calculation over 9 orders of magnitude. The data over theory plot for the same data is given in Fig. 5. The data points are in black for both rapidity bins and the systematic uncertainties are indicated by the yellow band. The systematics are largely dominated by the uncertainty on jet energy scale. The jet energy scale is determined using the p_T balance in photon and jet events where the electromagnetic energy scale is known using Z decaying into e^+e^-, and the photon and the jet are required to be back-to-back. The theory corresponds to NLO QCD calculations using the CTEQ6.1M parametrisation. The CTEQ6.1 parton distribution uncertainty (mainly due to the bad knowledge of the gluon density at high x) is given by the red dashed line, and the difference with the MRST2004 [7] parametrisation by the blue dotted line. The present uncertainties of the measurement do not allow a further constraint of the parton distribution. A significant improvement of the jet energy scale uncertainty is expected in the beginning of 2006 which will allow to constrain the high-x gluon density. Let us also note that a measurement at higher rapidity is also another way to be sensitive to the high-x gluon since pure gluon-gluon and quark-gluon jets are more present at higher rapidity than quark-quark processes. A preliminary measurement with a lower luminosity has already performed at lower luminosity and is being redone [8]. The measurement of the dijet mass cross section has also been performed by the DØ collaboration and will allow to put some new limits on compositeness in the near future since this measurement is sensitive to possible quark or gluon substructures [8]. The CDF collaboration performed a similar measurement of the inclusive jet p_T cross section using the k_T algorithm [9].

2.3. Measurement of the difference in azimuthal angles between jets

Another measurement which has been performed by the DØ collaboration is the measurement of the difference in azimuthal angle between the two leading jets in QCD events [10]. The azimuthal angle between the two leading jets is expected to be close to π for pure dijet events whereas the

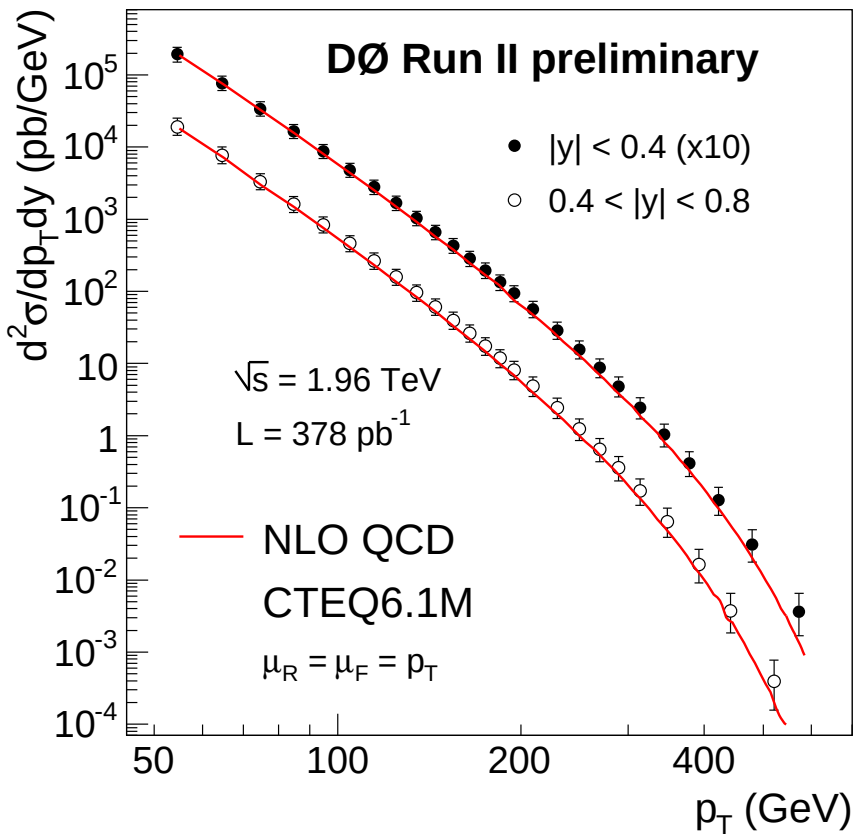

Fig. 4. Measurement of the inclusive jet cross section as a function of their transverse momentum from the DØ collaboration for two bins in rapidity.

angle will be less than π in the case of multiple jet events. The angle measurement is thus directly sensitive to higher order effects without measuring effectively the jet structure of the event. Furthermore, this measurement does not suffer too much from the jet energy uncertainty due to jet energy scale since it depends on angles and not directly on energy. The measurement of the relative differential cross section in azimuthal angle is shown in Fig. 6 in four different bins in jet transverse energy. The measurement is compared to LO and NLO calculation in dashed and full lines respectively. We notice a disagreement at low values of $\Delta\Phi$ with the LO calculation since the number of multijet events is too small at LO. NLO calculation agrees

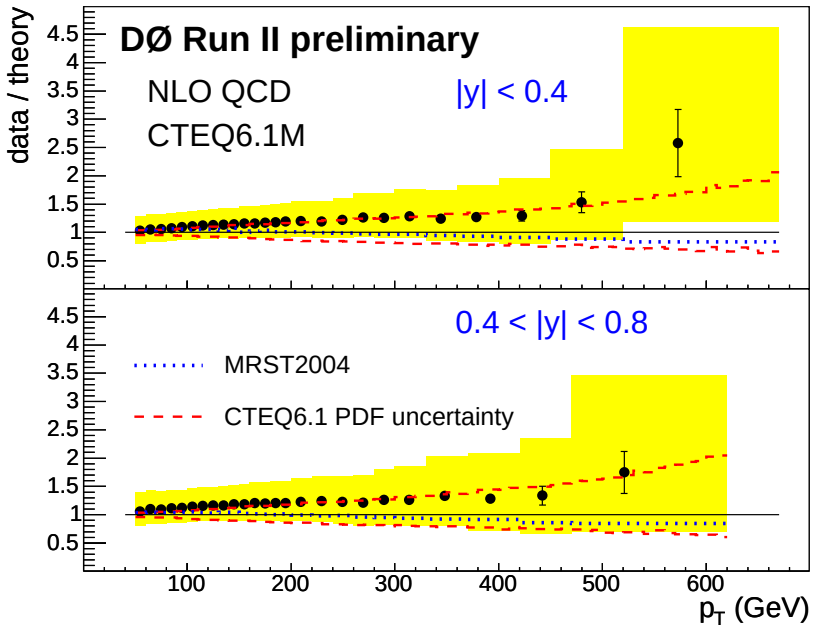

Fig. 5. Data over theory ratio for the inclusive jet cross section measurement from the DØ experiment.

nicely with the data except at very large $\Delta\Phi$ close to π where not enough soft radiation is produced. We also show the sensitivity of this measurement on Monte Carlo tuning in Fig. 7. The HERWIG [11] Monte Carlo shows a good agreement with data, whereas the default PYTHIA [12] shows some discrepancy. Increasing initial state radiation in PYTHIA (technically, PARP(67) was increased from 1. to 4.) solves the problem, and the sensitivity on this parameter is shown in Fig. 7 by the blue band. It is quite important to determine precisely the parton distributions in the proton and to tune the existing Monte Carlo to be able to obtain precise predictions at the LHC, which is fundamental to see some effects beyond the Standard Model, especially in the jet channels. We can quote in particular the importance of understanding the jet cross sections for R-parity violated SUSY or the search for higher dimensions.

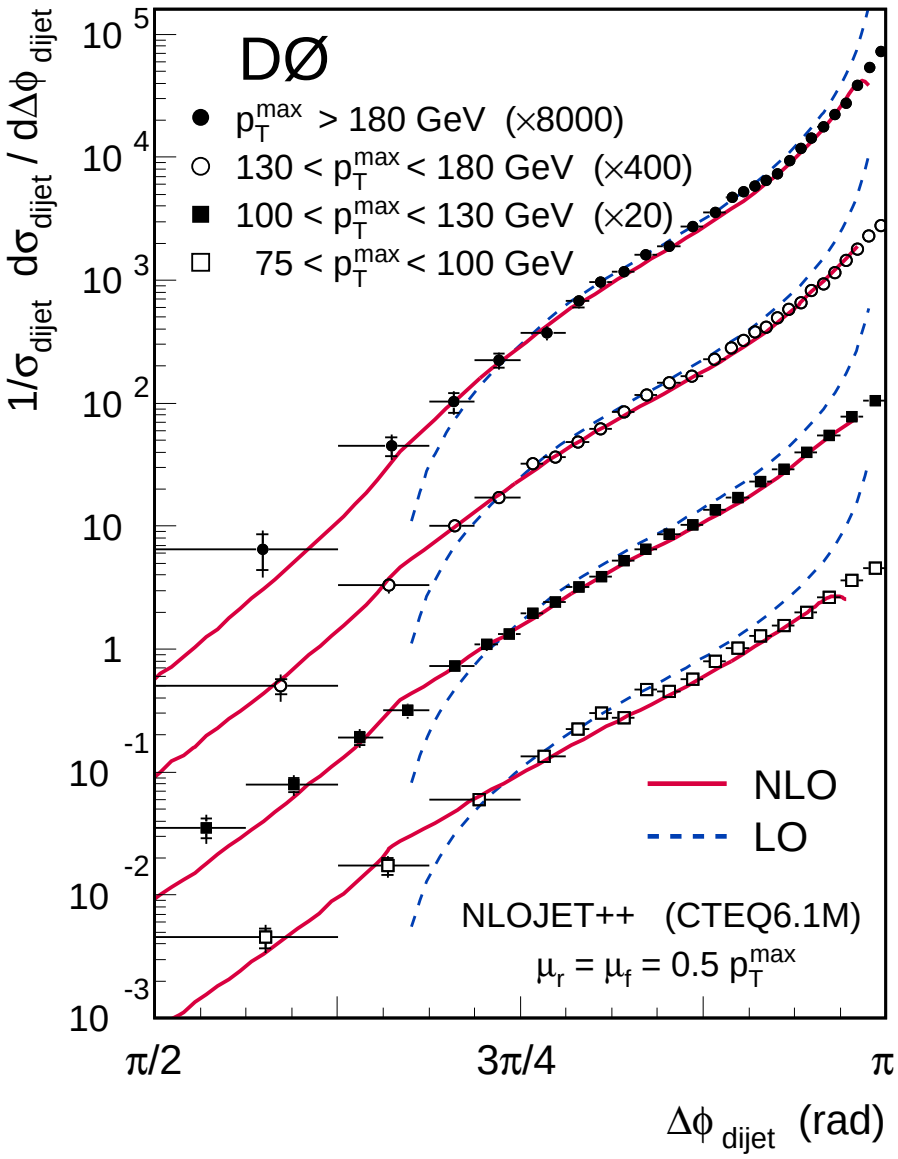

Fig. 6. Measurement of the difference in azimuthal angle between the two leading jets in multijet events (DØ collaboration).

2.4. Jet shape measurement

The CDF collaboration performed another measurement sensitive to the gluon and quark contents in the proton, as well as α_S and multi-gluon

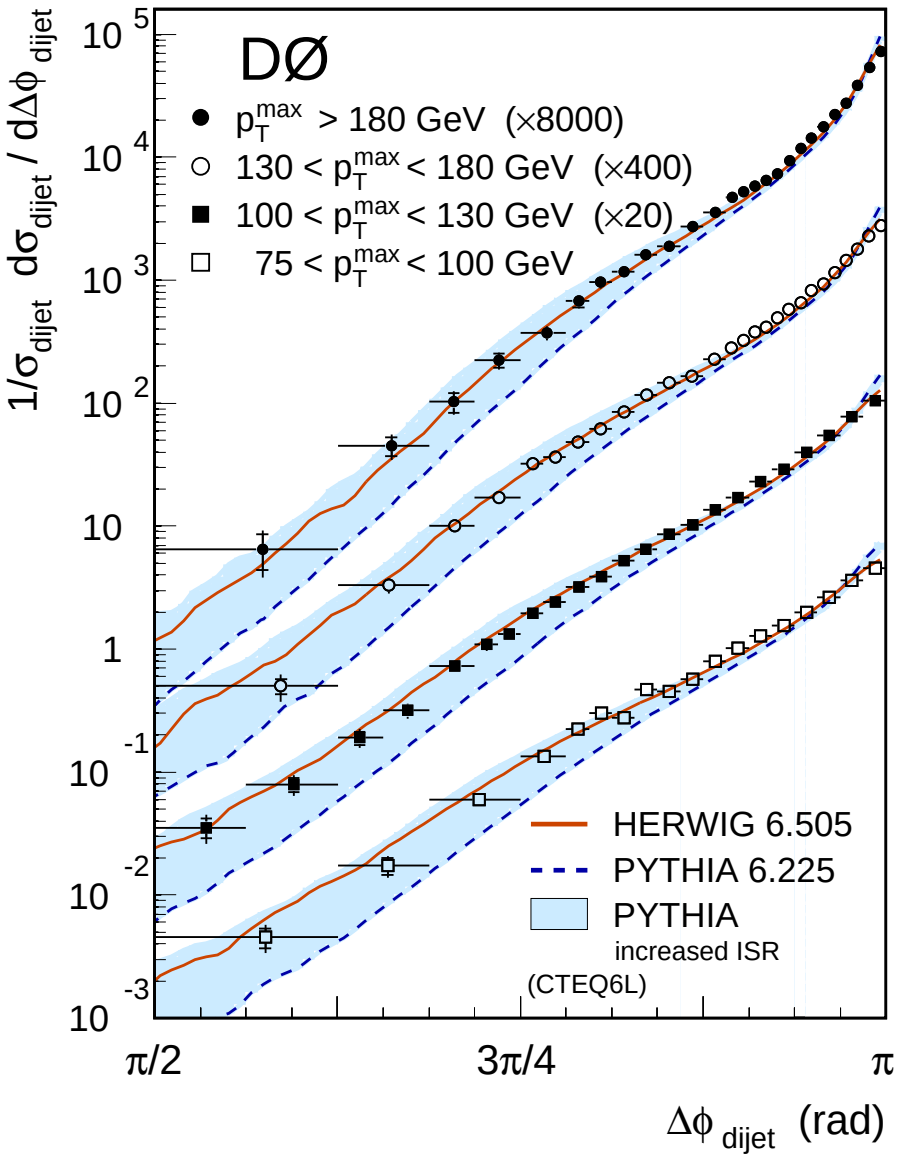

Fig. 7. Sensitivity of the measurement of the difference in azimuthal angle between the two leading jets in multijet events to MC tuning (DØ collaboration)

emission, namely the jet shape measurement. The measurement consists in

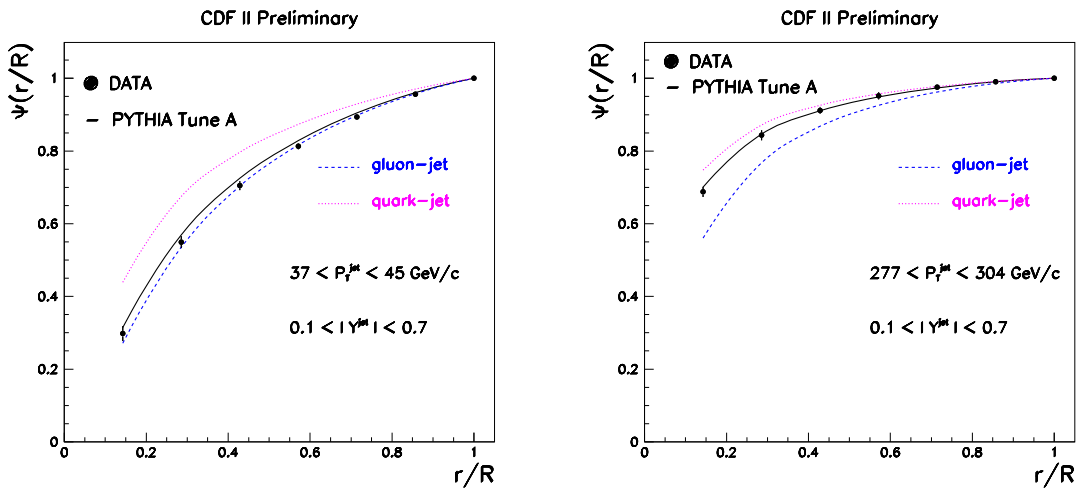

Fig. 8. Jet shape distributions for two bins in jet transverse momentum.

measuring $\Psi(r)$ defined as follows:

$$\Psi(r) = \frac{1}{N_{jets}} \Sigma_{jets} \frac{P_T(0,r)}{P_T^{jet}(0,R)}, \tag{1}$$

where the summation runs over the number of jets in the event (N_{jets}), and the jet radius is R. $\Psi(r)$ is a measurement of the repartion of transverse energy within the jet. Fig 8 shows the jet shape distributions for two different bins in jet transverse momentum, namely ($37 < p_T < 45$ GeV) and ($277 < p_T < 304$ GeV) for central jets ($0.1 < |y| < 0.7$). The CDF measurement extends to more p_T bins [13]. We also display in the same figure the expectations from the PYTHIA [12] Monte Carlo for gluon and quark jets. This measurement allows to determine the proportion of quark and gluon jets as a function of their transverse momentum. As expected, the lowest p_T jets are gluon process dominated whereas the higher p_T jets are quark process dominated.

2.5. Underlying events at the Tevatron

Fig. 9 shows a typical jet event at the Tevatron. The upper plots describes the hard scattering process where one observes the jet produced

in the event as well as the beam remnants. The lower plot displays what really happens at the Tevatron (or later on at the LHC). In addition to the hard scattering, we have initial and final state radiation which can produce additional jets in the event, and additional partonic interactions not related to the hard interaction (soft colour interactions can occur between the spectator partons in addition to the hard interaction). This results in additional energy measured in the detectors which are not related to the partonic interaction. It is important to understand this phenomenon if one wants to go back to parton level processes to measure the top mass, for instance. To study these "underlying events" (by opposition to the main hard scattering) the CDF collaboration measured the energy emitted outside the dijet hemisphere in clean back-to-back dijet events. For those events, one picks first the direction of the leading jet in the events, and measures the energy in the transverse region away from the leading jet. To avoid the particles included in both jets, only the energy between 60 and 120 degrees in azimuthal angles away from the leading jet is measured. This energy is dominated by underlying events, or in other words, by soft partonic interactions. The results were compared to the PYTHIA Monte Carlo [12] and found to be in good agreement [14] since PYTHIA was already tuned to previous run I CDF data. It is important to note that this tuning will have to be redone at the LHC aince it is not expected that the energy of underlying events will be independent of the center-of-mass energy.

3. Results on diffraction

Diffractive events are of special interest since they show undestroyed protons in the final state, and their mechanism is not yet fully understood. Mainly two kinds of models exist to describe diffraction: the first model assumes the existence of a colourless object, the Pomeron, which itself can be constituted of quarks and gluons, and the other one assumes that diffractive events are due to non perturbative string rearrangements in the final state (this happens at a much longer time scale than the hard interaction, at the time scale of hadronisation). We distinguish between single diffractive events and double pomeron exchanges which correspond to diffractive events on the proton or antiproton side only or on both sides.

3.1. Structure of the pomeron

Experimentally, there are two different ways to study diffractive events. The first way is to detect directly events where there is no colour exchange between the jet produced in the event and the proton in the final state, and to look for a gap in rapidity in the forward region away from the proton direction. The other way is to detect directly the proton in the final state

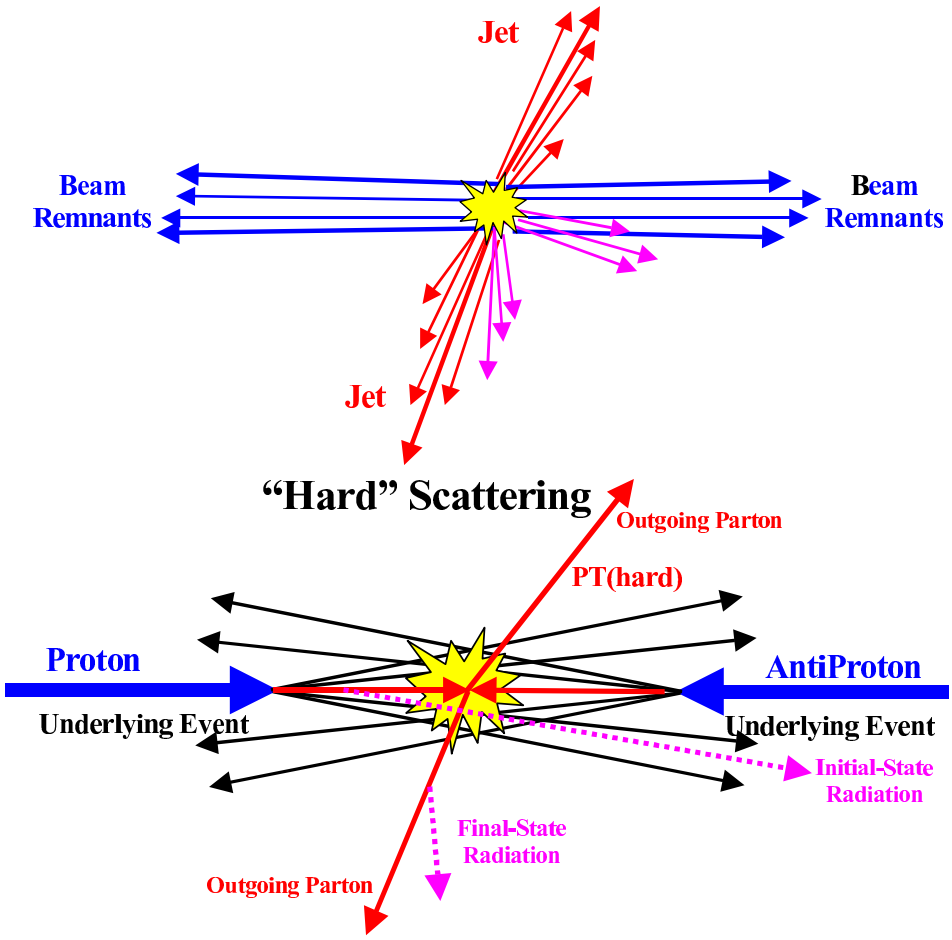

Fig. 9. Underlying events at the Tevatron.

in dedicated detectors far away from the main detector in the tunnel called roman pot detectors. The DØ and CDF collaborations installed this kind of detectors in the tunnels. To describe diffractive events, one introduces two additional kinematical variables: ξ is the fraction of the proton momentum carried by the non coloured object (the Pomeron), and β is the fraction of the pomeron momentum carried by the interacting parton (quark or gluon) inside the Pomeron if we assume a partonic structure of the Pomeron. By definition, $x_{bj} = \beta \times \xi$. The CDF and DØ "dipole" (close to the dipole magnets) roman pot detectors are located at about 58 m away from the main detector in the outgoing antiproton direction and are sensitive to t down to 0, and $0.02 < \xi < 0.05$. The DØ collaboration installed in addition

"quadrupole" roman pot detectors (close to the quadrupole magnets) in both outgoing proton and antiproton directions located at about 23 and 33 meters away from the main detector. These last detectors are sensitive to $|t| > 0.5$ GeV^2, and $10^{-3} < \xi < 3.10^{-2}$. The commission of these detectors was recently finished and new physics results are expected soon.

The percentage of single diffractive events was already measured by the DØ and CDF collaborations in Run I and found to be about 1% and depends on the exact process considered. The amount of diffractive events at HERA, the *ep* collider located at DESY, Hamburg, is close to 10%, which shows already that we cannot obtain the Tevatron results directly from the HERA data, or in other words, that there is no factorisation between *ep* and $p\bar{p}$ colliders. This can be due to additional soft interactions (soft gluon exchange) between partons in the final state which kill the rapidity gap or destroy the proton in the final state.

One important measurement on diffraction was performed in Run I by the CDF collaboration [15]. Using single diffractive events, (an anti-proton was tagged in the roman pot detector), the CDF collaboration was able to measure the gluon density in the Pomeron using dijet events. The CDF data points and their error bands in yellow are shown in Fig. 9. The results are compared directly to the expectations from the H1 diffractive DGLAP QCD fits in red full line. We notice that there is a discrepancy in normalisation by about a factor 10 between the CDF measurement and the HERA expectations (this corresponds to the different in the percentage of diffractive events between HERA and the Tevatron already mentionned). However, in a large domain in β, the shape of the gluon density is found to be similar which means that the same shape for the gluon density can be used to describe HERA and Tevatron data, as well as probably LHC data in the future. It is quite important to have precise measurements of the gluon and quark densities inside the pomeron if one wants to make precise predictions at the LHC [16].

Other measurements have been performed by the CDF collaboration [17] concerning the tests of factorisation at the Tevatron. It was found that factorisation holds almost in the full phase space at the Tevatron alone, and that the same x and Q^2 dependence has been found for inclusive or diffractive jet production.

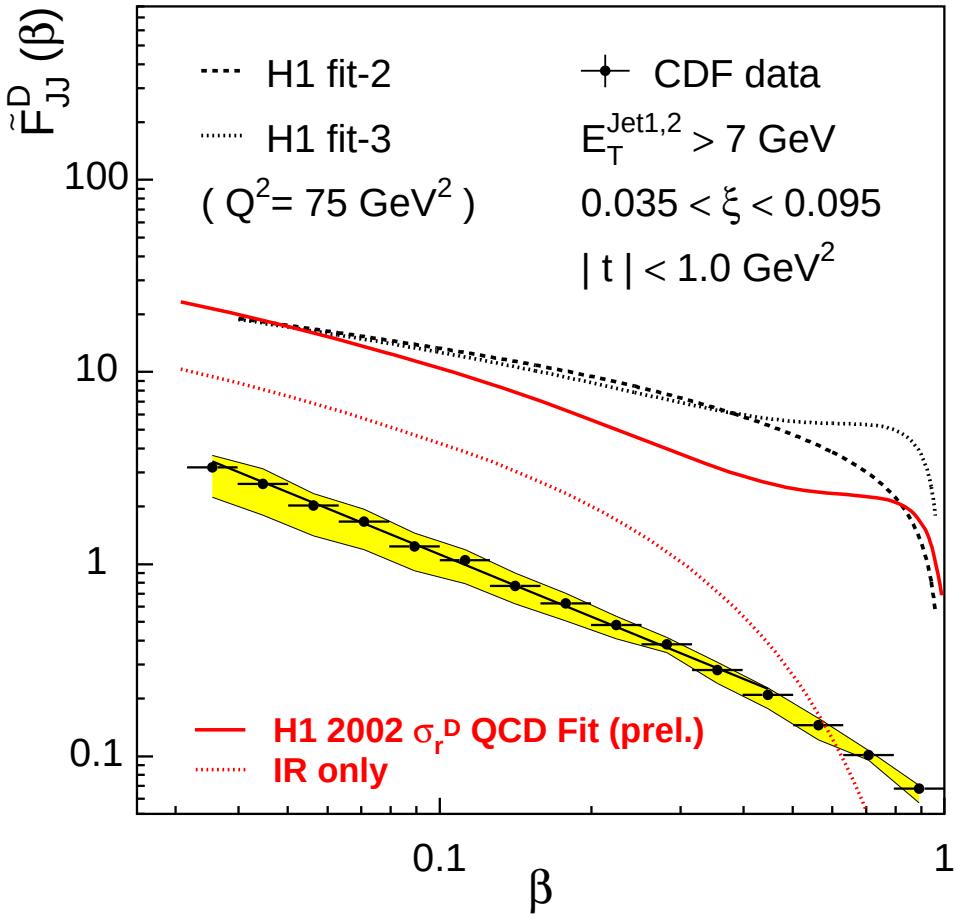

Fig. 10. Comparison between the gluon density measured at the Tevatron (CDF data points) and the one measured at HERA (result of the H1 QCD fit in full red line).

3.2. Search for diffractive exclusive production

Looking for the existence of exclusive events at the Tevatron is quite important for the LHC. If exclusive events exist, it could be a way to look for diffractive exclusive Higgs, top, or stop production at the LHC depending on the production cross section [18], since it is possible to reconstruct precisely the mass of the object produced diffractively using roman pot de-

tectors, using the so-called missing mass method, the total diffractive mass produced being equal to $M = \sqrt{\xi_p \xi_{\bar{p}} S}$. The CDF collaboration started to look for the eventual existence of exclusive events in the dijet channel. The results are shown in Fig. 11 for a low luminosity of 26 pb^{-1} (the actual accumulated luminosity by DØ and CDF is about 1 fb^{-1} and we can expect an update of these results very soon). The CDF data are divided in three different samples corresponding to single diffraction (triangles), and double Pomeron exchange (empty and full circle points requiring a different domain in rapidity for the gap: $5.5 < \eta < 7.5$ or $3.6 < \eta < 7.5$ for empty and full points respectively). The dijet mass fraction (the ratio of the dijet mass by the total diffractive mass in the event) is displayed in Fig. 11. Exclusive events are expected to appear at large dijet mass fraction since the full energy is used to produce dijets (there is no loss of energy in pomeron remnants). No enhancement is observed at high dijet mass fraction which is compatible with the tail of the inclusive distribution, but the cross section for exclusive production is expected to be small. It will be quite interesting to see the results with higher luminosity. Other methods can also be developped to look for exclusive events like measuring the correlation between $\log 1/\xi$ and the size of the rapidity gap which is larger for exclusive events, the ratio of the dilepton to diphoton cross sections which should show an enhancement at high diphoton-dilepton mass if exclusive events exist, or the ratio between b and light jet diffractive production [19].

Another method is to look for diffractive χ_C production. Unfortunately, the acceptance for such low mass objects to be detected in roman pot detectors is small and the selection requires the existence of rapidity gaps. The diffractive mass has to be computed using the central calorimeter without benefitting from the good resolution of the roman pot detectors. The CDF collaboration looked for χ_C^0 decaying into dimuon and a photon, and no further activity in the central detector was requested to ensure the exclusiveness of the process. A few exclusive candidate events were found but it is difficult to determine precisely the cosmic contamination [20].

4. Top physics

Top physics is one of the hottest subjects at the Tevatron, which is the only place where the top quark can be studied before the start of LHC. The top quark was indeed discovered at the Tevatron Run I in 1995 by the DØ and CDF collaborations. Compared to the other quarks, it has a much higher mass (its mass is about 174 GeV which is 40 times the bottom quark mass). Due to its mass, the top quark life time is very short (about 10^{-25}s), and the top quark decays before hadronisation. In Fig. 12, the schematic production and decay of a typical $t\bar{t}$ event is displayed. The production cross

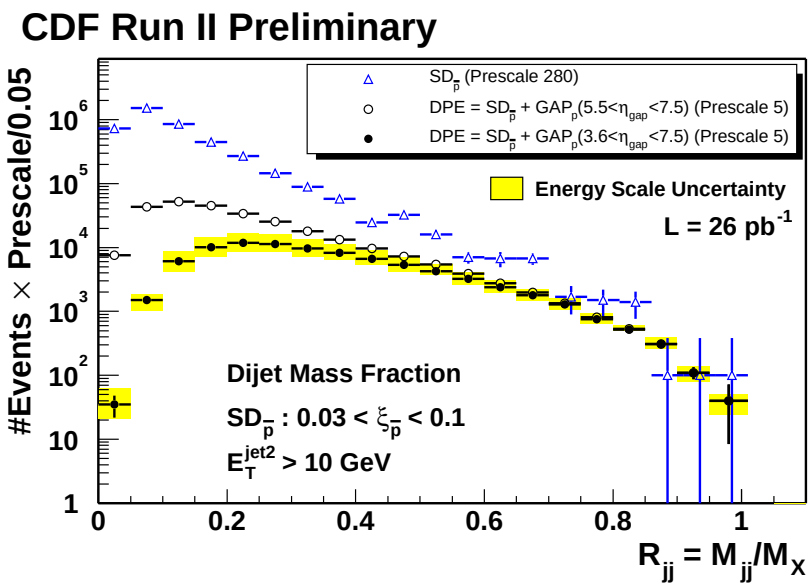

Fig. 11. Dijet mass fraction measured in the CDF detector for double Pomeron exchange.

section at the Tevatron is of the order of 6 pb, 85% of which are produced via a $q\bar{q}$ interaction, and 15% via a gg one. The top quark decays into a W and a b quark in 100% of the cases since V_{tb} is much greater than V_{ts}, V_{td}. The W can decay either leptonically as indicated in the figure or into 2 jets (quarks $u\bar{d}$). A typical topology to look for $t\bar{t}$ events is a multijet event (6 jets, 2 can be b-tagged), or a multi jet and lepton event with missing transverse energy coming from the W decay.

4.1. Measurement of the top quark mass

The measurement of the top quark mass is a fundamental test of the Standard Model. The radiative corrections to the Standard Model predictions of electroweak measurements are dominated by the value of the top mass, and a precise measurement of the top mass is needed to constrain the electroweak tests of the Standard Model and the Higgs boson mass. The measurement of the top mass depends first on the identification of the $t\bar{t}$ events by requiring a leptonic, multijet (at least 4) event, and missing transverse energy. The background to this topology can be further reduced requiring some jets to be b-tagged. The mass measurement is also very sensitive the determination of the jet energy scale. One of the easiest methods

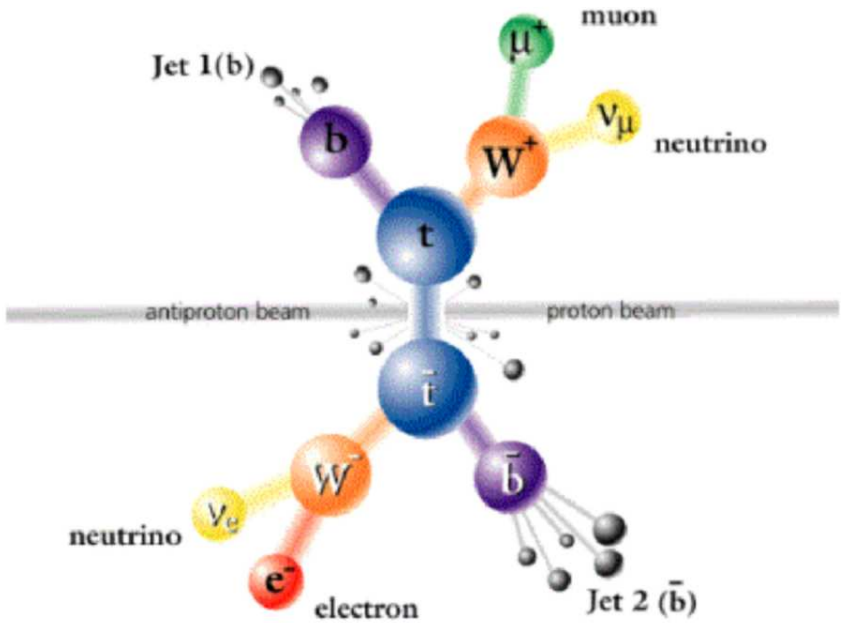

Fig. 12. Scheme of a $t\bar{t}$ event.

to determine the top mass is to use the template method. The basic idea is to compute a χ^2 between data and Monte Carlo simulations assuming different values of the top mass. In fact, the method is slightly more complicate: it is for instance possible to constrain the jet energy scale by constraining the measurement of the W mass in data to be in agreement with the world average since the W mass is already known precisely. The different Run II measurements of the top quark mass (at the time of the summer school) [21] are given in Fig. 13 for the DØ and CDF collaborations. By comparison, the Run I average was 178 ± 4.3 GeV and the best single top mass measurement was performed in the lepton and jet channel by the DØ collaboration [22] (180.1 ± 5.3 GeV). A precision on the top mass a bit higher than 1 GeV is expected by the end of Run II at the Tevatron. The new Run I top mass led to the prediction of the Higgs boson mass of $(114 + 69 - 45)$ GeV using electroweak fits. Reducing the uncertainty on the top mass will allow to reduce its large uncertainty.

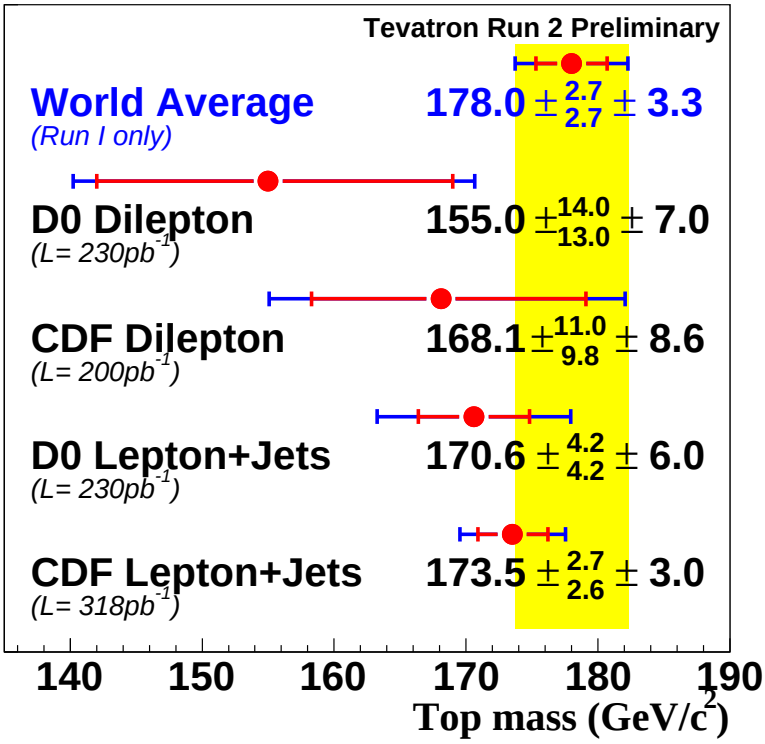

Fig. 13. Measurement of the top quark mass.

4.2. Measurement of the $t\bar{t}$ production cross section

The analysis of the $t\bar{t}$ events described in the previous paragraph leads directly to a measurement of the $t\bar{t}$ production cross section and can be compared directly to the prediction of the Standard Model. Many different methods (dilepton, lepton and jet, multi jet channels) are used by the CDF and DØ collaborations [23]. The combined result for the CDF collaboration is given in Fig. 14.

4.3. Search for single top production

Another way to produce the top quark predicted by the Standard Model is the electroweak single production, where the top quark is produced via a W. This process has not yet been observed, but a limit at 95% CL was set

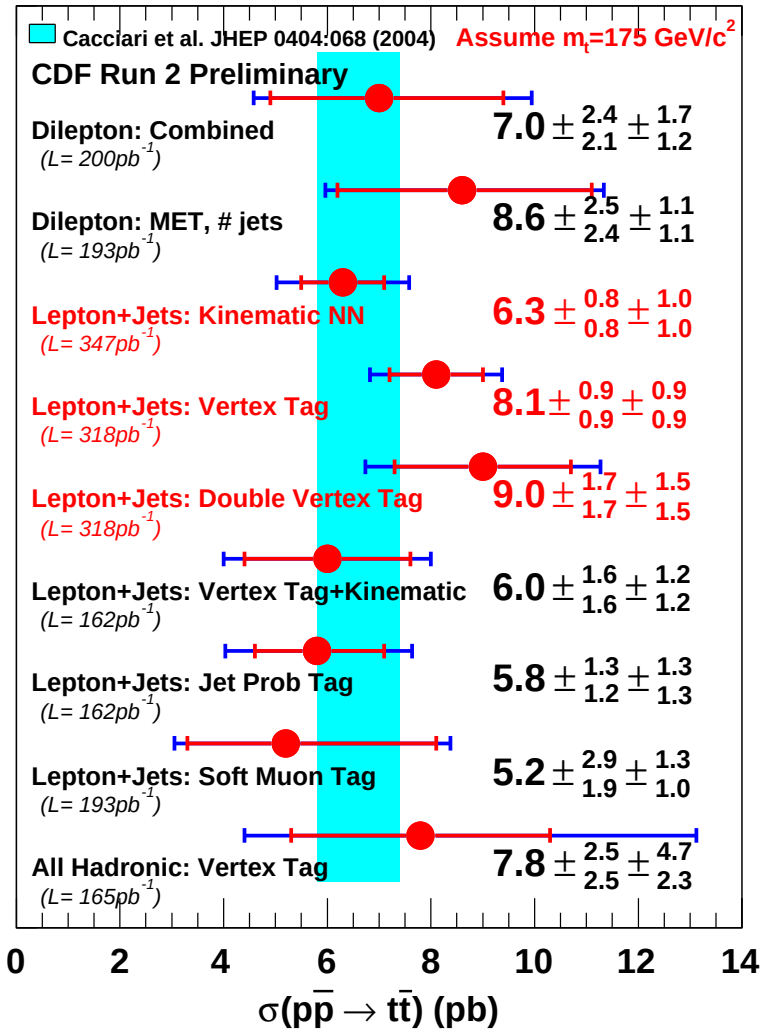

Fig. 14. $t\bar{t}$ production cross section (CDF collaboration). The DØ collaboration shows similar results.

by the DØ collaboration on the production cross section at 6.4 pb in the s-channel and 5 pb in the t-channel [24]. The limit is now close to the cross section predicted by the Standard Model and an observation could come soon. The advantage of that process is to study the CKM matrix element V_{tb}, the top width and the Wtb coupling.

5. Electroweak physics

5.1. Measurement of W and Z production cross sections

Z and W bosons can be produced directly by quark interactions at the Tevatron. To obtain a lower background, one measures the W and Z cross sections when the Z or the W decays into dileptons or lepton and neutrino respectively. The CDF and DØ results are given in Fig. 15 and Fig. 16 for Z and W production respectively [25]. The results obtained in Run I (center-of-mass energy of 1.8 TeV) are displayed together with the new Run II results (center-of-mass energy of 1.96 TeV) and compared with the Standard Model expectation (full line). The data points are not put all at either 1.8 or 1.96 TeV to be able to distinguish between them. The different leptonic decays of the Z or W are shown (electron, muon or tau) and we also note the good agreement between the measurements.

Another important measurement to be performed at the Tevatron is the W mass. Some update on this subject are expected in the near future. The measurement requires a very good understanding of the systematics to be able to obtain a world competitive measurement.

5.2. W asymmetries

The W asymmetries have been measured by the CDF collaboration. The advantage of this measurement is that it is sensitive to u and d contents of the proton. In average, u quarks carry more proton momentum than d quarks. As a consequence, the rapidity distribution for W^+ is different from the one for W^-. Namely, W^+ which are produced mainly by u and $\bar{d}$ interaction receive a boost in the u direction, and W^- which are produced by d and $\bar{u}$ in the $\bar{u}$ direction. This explains why the rapidity distribution for W^+ (respectively W^-) has the tendency to be shifted towards positive (respectively negative) values of rapidity. The CDF collaboration measured the W asymmetries defined as follows:

$$A(y) = \frac{d\sigma(W^+)/dy - d\sigma(W^-)/dy}{d\sigma(W^+)/dy + d\sigma(W^-)/dy} \sim \frac{d}{u} \tag{2}$$

which gives a direct access to the ratio of d and u quark densities. The result is shown in Fig. 17 for a transverse energy bin between 35 and 45

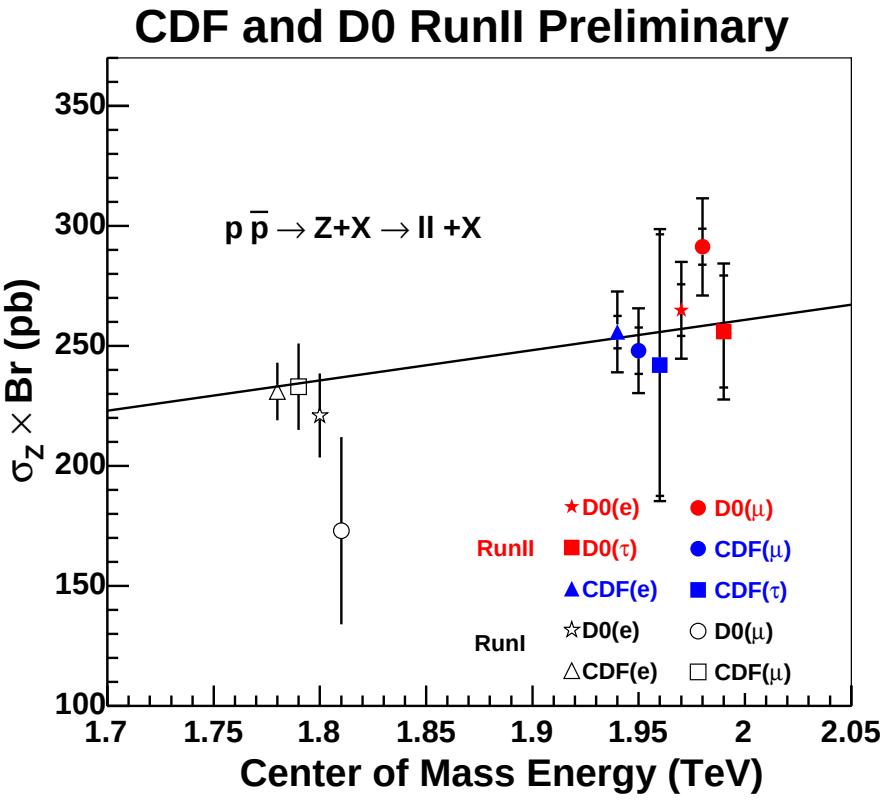

Fig. 15. Z production cross section.

GeV as a function of W rapidity. The expectations from the CTEQ and MRS distributions are also given [26]. We see that the main differences occur at high rapidity. With more accumulated luminosities, it will possible to perform the same measurement at higher energy which will give more sensitivity on the quark densities.

6. B physics

Many results have been published already by the CDF and DØ collaborations concerning B physics. Due to the lack of time, we will cover only a few topics. Other results can be found on the web pages of the collaborations [27].

A general plot showing the resonances appearing in the dimuon systems can already give a feeling on the excellent mass resolution obtained by the

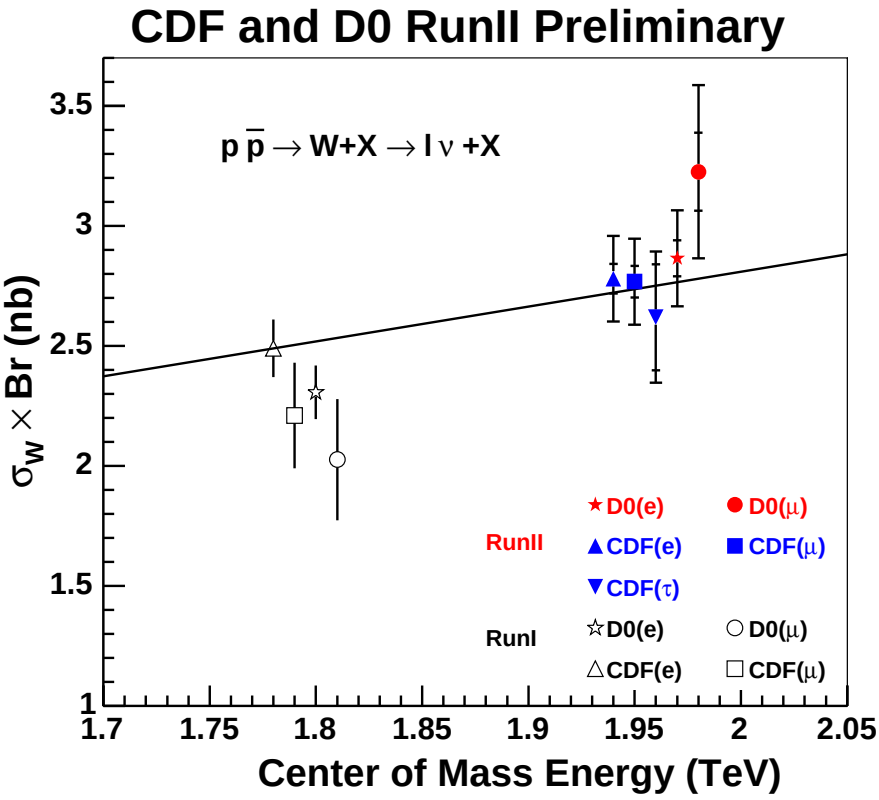

Fig. 16. W production cross section.

DØ and CDF detectors due to their tracking and silicon detectors. Fig. 18 displays the ω, Φ, J/Ψ, Ψ' and Υ resonances observed by the DØ collaboration in the dimuon system. Other resonances such as B^+, Φ, or Λ_b, ... have also been studied by the DØ and CDF collaborations [27].

The DØ collaboration also observed the $X(3872)$ resonance [28] in the J/Ψ $\pi^+\pi^-$ channel as it is shown in Fig. 19. The mass difference between $X(3872)$ and J/Ψ has been found to be 774.9 $\pm 3.1(stat.) \pm 3.0(syst.)$MeV.

7. New phenomena

The new phenomena studies are done by the DØ and CDF collaborations mainly in the SUSY framework. We defined the so-called R-parity which is $(-1)^{2j+B+L}$ where j, B and L stand for spin, baryon and lepton numbers. Standard Model (respectively SUSY) particles show $R = 1$ (respectively

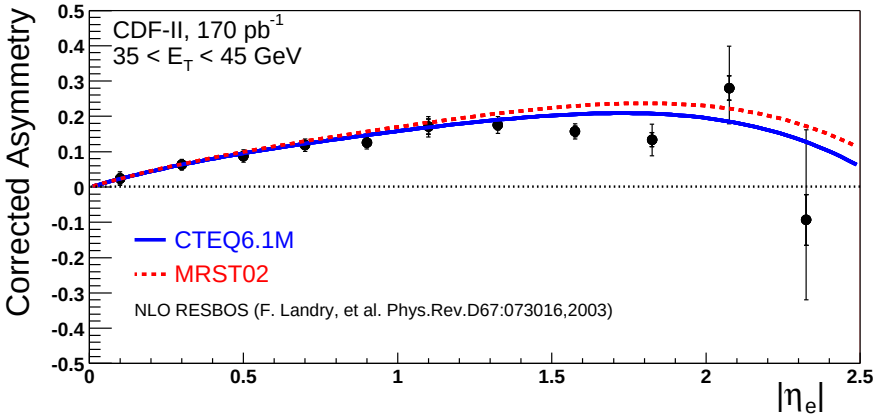

Fig. 17. W asymmetries (CDF collaboration).

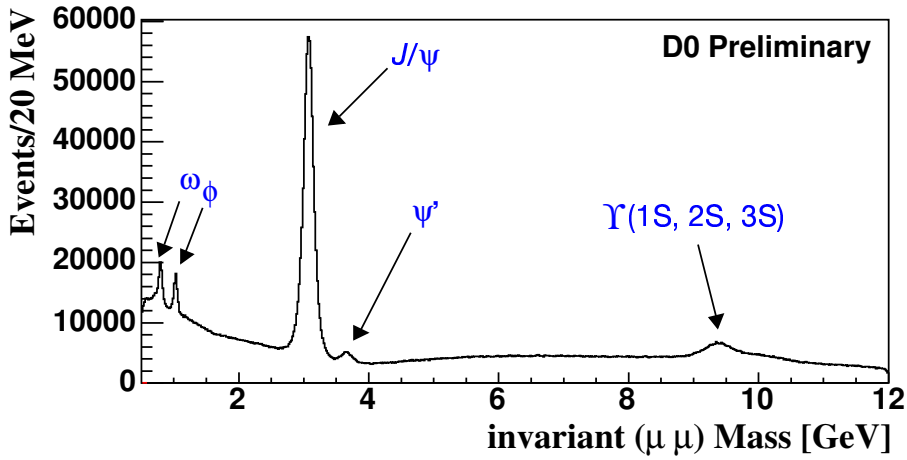

Fig. 18. Dimuon resonances observed by the DØ collaboration.

$R = \pm 1$). The experimental signatures to look for SUSY particles are different if R-parity is conserved or violated. When R parity is conserved, SUSY particles are produced in pairs, and they decay into the lightest SUSY particle (LSP) which escapes undetected. Experimentally, this induces some missing transverse energy which can be detected. On the contrary,when R parity is not conserved, the LSP decays, and the experimental signature is an event with multi-lepton, multi-jets, with little missing transverse energy, and the process often includes lepton flavour violating decays.

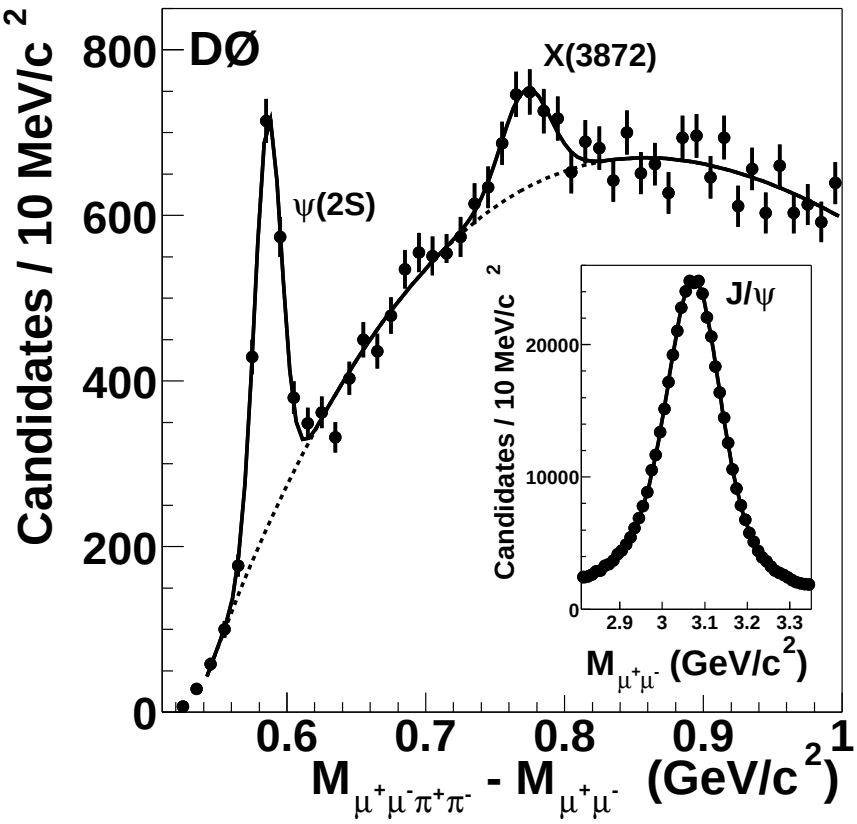

Fig. 19. Observation of $X(3872)$ by the DØ collaboration.

Before describing the search for new phenomena, let us give some feelings about the cross section we are concerned with. Typical jet production cross section at the Tevatron are of the order of 10^{12} fb (10^{11} fb for b-jets), whereas the W and top typical cross sections are in the order 10^7 and a few 10^3 as we mentioned in previous paragraphs. The present limits on SUSY particle production cross section lay in the region of 10^4 fb for squark production and a few tenths of fb for sleptons. We already see that the main problems of new phenomena analysis will be to get rid of the huge background without losing too many new phenomena events since they are expected to be rare.

We will not give here a complete exhaustive list of all new phenomena results but rather focus on three particular ones. All results from the DØ and CDF collaborations can be found on their web pages [29].

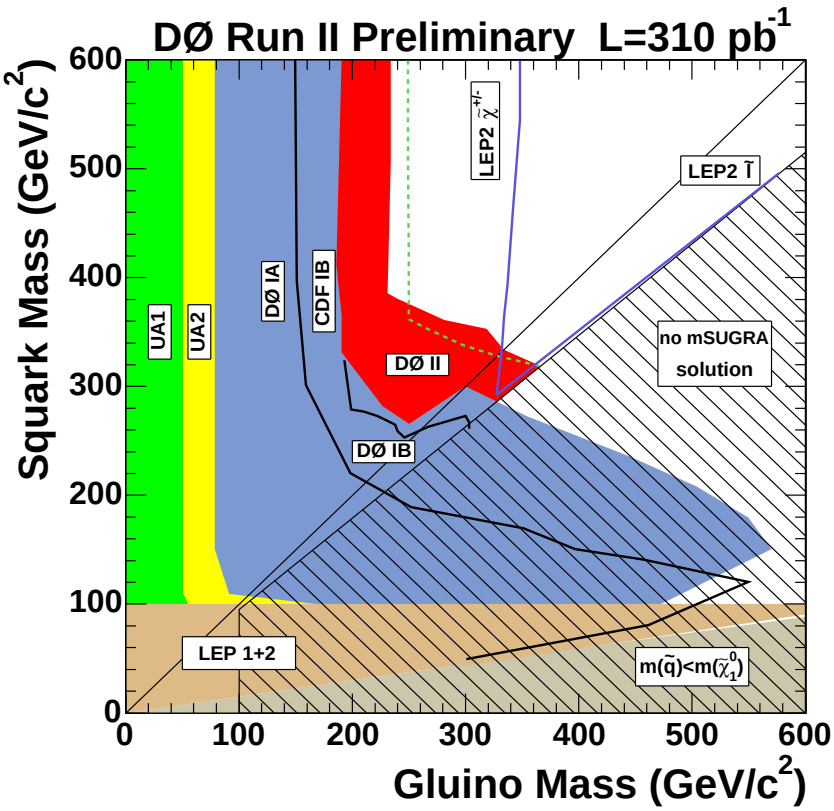

Fig. 20. Limits in the squark-gluino mass plane obtained by the DØ collaboration

7.1. Squarks and gluinos

Squarks and gluinos can be produced directly by pairs at the Tevatron via a $q\bar{q}$ interaction. The squarks decay into the LSP (assumed to be the $\tilde{\chi}_1^0$) and a quark. The topology for squark pair production will be 2 jets and missing transverse energy. Similarly, the topology for squark gluino or gluino pair production is respectively two jets and missing transverse energy or three jets and missing transverse energy. No signal has been found in this channel and the limit has been obtained by the DØ collaboration in the squark-gluino mass plane [30] for 310 pb^{-1} as shown in Fig. 20. The previous limits from LEP and Tevatron Run I are also displayed on the figure.

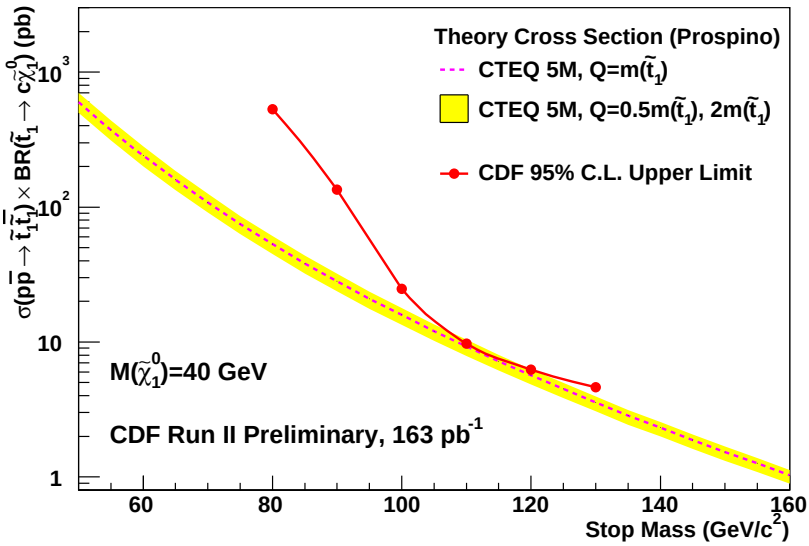

Fig. 21. Limits on the stop pair production cross section times branching ratio by the CDF collaboration.

7.2. Stop production in mSUGRA

The CDF collaboration studied the production of stop pair in minimal supergravity (mSUGRA) scenario. Stops are produced in pair as in the previous squark production. The stop (assumed to be the next lightest supersymmetric particle) is assumed to decay into $c\tilde{\chi}_1^0$ where the $\tilde{\chi}_1^0$ is assumed to be the LSP. The selection is thus to require two reconstructed jets coming from the c quark and missing transverse energy from the LSP. The study is made for different mass values of the LSP, and as an example, we show the results for a LSP mass of 40 GeV in Fig. 21. The CDF limit is displayed in full and the stop production cross section in dashed line for the CTEQ5M parametrisation [31].

7.3. Resonant sparticle production with violated R-parity

When R-parity is violated, it is possible to produce sparticles in the s-channel in a resonant mode [32]. For instance, it is possible to produce smuons from d and $\bar{u}$ quarks and the so-called λ'_{211} coupling. In the same way, the LSP can decay via another R-parity violating coupling. New limits have been established by the DØ collaboration for resonant sparticle pro-

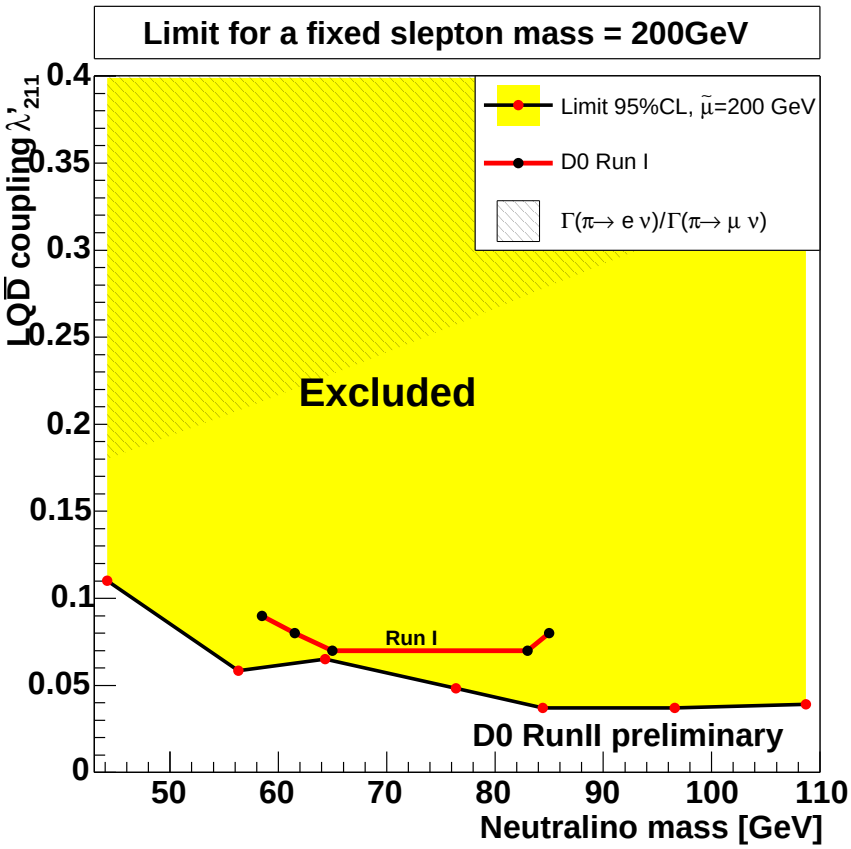

Fig. 22. Limits on the λ'_{211} coupling as a function of the neutralino mass for a fixed slepton mass of 200 GeV from the DØ collaboration.

duction for the λ'_{211} coupling for different neutralino and slepton masses. As an example, we display in Fig. 22 the limits on the λ'_{211} coupling as a function of the neutralino mass for a fixed slepton mass of 200 GeV [33], the Run I result being indicated for reference.

7.4. Search for Higgs boson

A hot but difficult topic for the Tevatron is the search for neutral Higgs bosons. Predictions have been made on the sensitivity to look for Higgs bosons in the next years when luminosity increases and are given in Fig. 23. These results will strongly depend on the detector performances since the background is very high in all channels and the search for Higgs boson quite

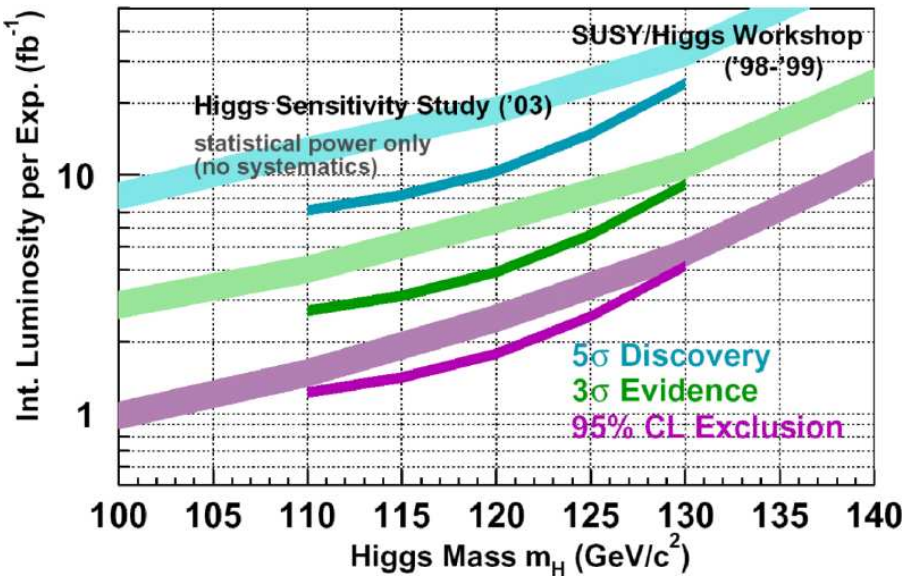

Fig. 23. Prospects to search for Higgs bosons at the Tevatron.

challenging. The large error band shows the expectations for a 5σ dicovery, 3σ evidence, and a 95% CL limit as a function of the Higgs mass from an analysis of the Higgs sensitivity study working group [34] (the smaller band shows the previous results). However these results do not include systematic errors but only statistical ones and are thus optimistic.

8. Conclusion

In these lectures, we have discussed many preliminary results from the Tevatron on QCD, diffraction, electroweak, top and B physics, and new phenomena. Much progress is expected in the future with the increase of luminosity (this will benefit directly to new phenomena studies and the search for Higgs bosons) and a better understanding of systematics which are often dominated by the uncertainty on jet energy scale (QCD cross section measurements and constraint on the parton distributions, electroweak physics and the W mass measurement, top physics and the top mass measurement allowing to constrain further the standard model and the mass of the Higgs boson).

Acknowledgments

The author thanks the organisers of the Zakopane Summer School for financial support and Jochen Cammin and Robi Peschanski for a careful reading of the manuscript.

REFERENCES

[1] DØ Collab., hep-physics/0507191, Fermilab-Pub-05/341-E., subm. to Nucl. Instr. and Methods

[2] G. Altarelli and G. Parisi, Nucl. Phys. **B126** 18C (1977) 298; V. N. Gribov and L. N. Lipatov, Sov. Journ. Nucl. Phys. (1972) 438 and 675; Yu. L. Dokshitzer, Sov. Phys. JETP. **46** (1977) 641.

[3] H1 Coll., Eur. Phys. J **C30** (2003) 1; ZEUS Coll., Phys. Rev. **D67** (2003) 012007.

[4] DØ Coll., D0 conference note 4751.

[5] J. Pumplin et al., JHEP **0207** (2002) 12; D. Stump et al., JHEP **0310** (2003) 46.

[6] Z. Nagy, Phys. Rev. Lett. **88** (2002) 122003; Z. Nagy, Phys. Rev. **D68** (2003) 094002.

[7] A. D. Martin et al., Phys. Lett. **B604** (2004) 61.

[8] DØ Coll., D0 conference note 4382 (for all conference notes: see http://www-d0.fnal.gov/Run2Physics/WWW/results.htm).

[9] CDF Coll., see http://www-cdf.fnal.gov/physics/new/qcd/inclusive05/ index.html, http://www-cdf.fnal.gov/physics/new/qcd/ktjets/ktjets.html.

[10] DØ Coll., Phys. Rev. Lett. **94** (2005) 221801.

[11] G. Marchesini et al., Comp. Phys. Comm. **67** (1992) 465; G. Corcella et al., JHEP **0101** (2001) 010.

[12] T. Sjöstrand et al., Comp. Phys. Comm. **135** (2001) 238.

[13] CDF Coll., see http://www-cdf.fnal.gov/physics/new/qcd/shapes/shapes.html.

[14] CDF Coll., see http://www-cdf.fnal.gov/physics/new/qcd/run2/ue/chgjet/ index.html; CDF Coll., Phys. Rev. **D70** (2004) 072002.

[15] CDF Coll., Phys. Rev. Lett **84** (2000) 5043.

[16] M. Boonekamp, R. Peschanski, C. Royon, Phys. Rev. Lett. **87** (2001) 251806; Nucl. Phys. **B669** (2003) 277; M. Boonekamp, R. Peschanski, A. De Roeck, C. Royon, Phys. Lett. **B 550** (2002) 93; for a review see: C. Royon, Mod. Phys. Lett. **A18** (2003) 2169, and references therein.

[17] CDF Coll., see http://www-cdf.fnal.gov/physics/new/qcd/run2/diffractive/ diff_bless/run2_diff_bless.html

[18] M. Boonekamp, J. Cammin, R. Peschanski, C. Royon, preprint hep-ph/0504199; M. Boonekamp, J. Cammin, R. Peschanski, C. Royon, S. Lavignac, preprint hep-ph/0506275; M. Boonekamp, R. Peschanski, C. Royon,

Phys. Lett. **B598** (2004) 243; A. Kupco, R. Peschanski, C. Royon, Phys. Lett. **B606** (2005) 139.

[19] M. Boonekamp, R. Peschanski, C. Royon, Phys. Lett. **B598** (2004) 243 and references therein.

[20] CDF Coll., see http://www-cdf.fnal.gov/physics/new/qcd/chi_c/prelim_chic/exc_chic.html

[21] DØ Coll., conference notes: 4574, 4874, 4728, 4725 and 4892; CDF Coll., see http://www-cdf.fnal.gov/physics/new/top/top.html

[22] DØ Coll., Nature **429** (2004) 638.

[23] DØ Coll., Phys. Lett. **B626** (2005) 55; Phys. Lett. **B626** (2005) 45; Phys. Lett. **B626** (2005) 35; CDF Coll., Phys. Rev. **D72** (2005) 052003; Phys. Rev. **D72** (2005) 032002; Phys. Rev. **D71** (2005) 052003; Phys. Rev. **D71** (2005) 072005

[24] DØ Coll., Phys. Lett. **B622** (2005) 265; CDF Coll., Phys. Rev. **D71** (2005) 012005.

[25] DØ Coll., conference note 4573, 4750, 4403; DØ Coll., Phys. Rev. Lett. **94** (2005) 151801; CDF Coll., Phys. Rev. Lett. **94** (2005) 091803; see http://www-cdf.fnal.gov/physics/ewk/.

[26] CDF Coll., Phys. Rev. **D 71** (2005) 051104.

[27] DØ Coll., see http://www-d0.fnal.gov/Run2Physics/WWW/results/b.htm; CDF Coll., see http://www-cdf.fnal.gov/physics/new/bottom/bottom.html

[28] DØ Coll., Phys. Rev. Lett. **93** (2004) 162002; CDF Coll., Phys. Rev. Lett. **93** (2004) 072001.

[29] DØ Coll., see http://www-d0.fnal.gov/Run2Physics/WWW/results/np.htm; CDF Coll., see http://www-cdf.fnal.gov/physics/exotic/exotic.html.

[30] DØ Coll., conference note 4737.

[31] CDF Coll., http://www-cdf.fnal.gov/physics/exotic/r2a/20041028.stop_ccmet/.

[32] F. Déliot, G. Moreau, C. Royon, Eur. Phys. J. **C19** (2001) 155; F. Déliot, G. Moreau, C. Royon, M. Chemtob, E. perez, Phys. Lett. **B475** (2000) 184 and references therein.

[33] DØ Coll., conference note 4535.

[34] CDF and DØ Coll., FERMILAB PUB-03/320-E